Laser-related effects on shock wave propagation

C D Gregory, C Courtois, I M Hall, J Howe, N C Woolsey

Department of Physics, University of York, Heslington, York, YO10 5DD, UK

D M Chambers

AWE Aldermaston, Reading, RG7 4PR, UK

Main contact email address: *cdg104@york.ac.uk*

Introduction

The propagation of laser-driven shock waves in gases has been studied extensively, for example[1-3]. These studies have typically focussed upon the late time dynamics of such shocks, after the evolution into a blast wave. Once a blast wave has formed any non-uniformities initially present have been lost, and the expansion is dependent only upon the initial energy density of the system. Recent work has indicated that the laser passage through the background gas can dramatically affect the evolution of the experiment, which can have important consequences for the physics of interest[4]. In this experiment the Astra laser was used to ablate a solid aluminium target in a background gas of nitrogen, causing a shock wave to form. In the early times studied here, the shock has not decayed into a blast wave, and the effect of the laser passage can clearly be seen. The pulse appears to form a low-density channel through which the shock can propagate at an enhanced speed.

Experiment

The experiment was performed using the Astra laser to focus 3ps, 400mJ, 800nm laser pulses onto a solid aluminium target, at an angle of 10^o to the target normal. The focal spot diameter was either 15µm or 100µm, resulting in an intensity on target of either 7x10^{16} Wcm^{-2} or 1x10^{15} Wcm^{-2} respectively. The vacuum chamber was evacuated and then back-filled with nitrogen gas to a pressure of between 10mbar and 100mbar.

The laser interaction with the solid target generates a large flux of x-rays, which ionise the background gas ahead of the ablated plasma plume. The ablated aluminium then streams away from the target surface, initially undergoing a brief period of supersonic free-expansion, until it begins to collide with the ambient plasma. These collisions cause the aluminium to sweep up the nitrogen plasma, leading to a pile up of mass at the ablation front. The result is a deceleration of the expansion, and the formation of an approximately spherical shock wave.

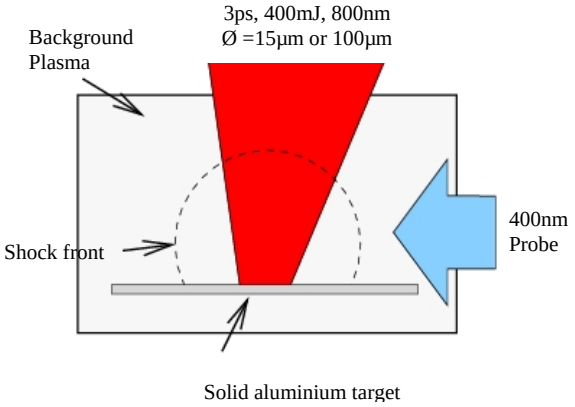

Figure 1. The experimental set-up. The Astra laser was incident at an angle of 10^o to the target surface. Ablated aluminium launched a shock wave into the ambient nitrogen gas. A 400nm probe beam was used to diagnose the experiment.

A portion of the main laser beam (~5mJ) was separated and frequency doubled to 400nm. This was then used to probe the experiment in a direction perpendicular to the plasma expansion, providing 3ps snapshots of the shock wave evolution at variable times of up to 13ns after the arrival of the drive pulse, see Figure 1.

Quantitative measurements of the electron density, n_e were made using interferometry, and shadowgraphy was used to determine the position and structure of the shock front.

Results

Figure 2 shows typical shadowgrams from experiments with 100µm and 15µm focal spots. In both cases the background gas pressure was 70mbar and the image was captured 4ns after the arrival of the main laser pulse. The main laser is incident from the top of the image, and the probe beam is in the direction out of the page. The aluminium target can be seen at the bottom of the image. The dark region of the expansion next to the target surface is below critical density for the probe beam, but the n_e in this region is sufficient to refract the beam out of the collection angle of the diagnostic.

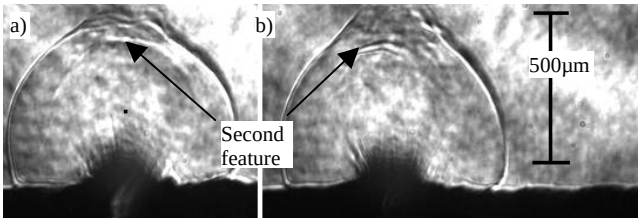

Figure 2. Shadowgrams taken at a probe delay of 4 ns, and with an ambient pressure of 70mbar. Focal spot size of a) 100µm and b) 15µm. A second density feature can be seen in both cases.

The shock front is seen to be uniform and approximately spherical at angles greater than ~ 30^o to the target normal direction, while the portion of the shock front which travels back through, or close to, the laser entrance cone is significantly altered. With a 100µm focal spot this effect is seen as a slight bump on the shock front, with a secondary density feature close behind. In the 15µm spot case the bump is more prominent, and a larger separation between the shock front and the density feature is observed.

The shock positions for background pressures of 30mbar to 100mbar, and for the two different focal spot sizes, are plotted in Figure 3 (at pressures lower than 30mbar the shock front cannot be clearly seen in the region of the laser cone). The shape of the shock at 4ns appears approximately independent of the laser focal spot size, except for the region around the laser axis, as described above. This difference is particularly apparent for nitrogen pressures of 50mbar and 70mbar. The bump feature has also been observed at probe delays of 13ns.

As the shock moves away from the target surface it accrues mass as it snowploughs up the ambient gas, resulting in a deceleration of the shock. By increasing the gas pressure the mass swept up by the shock as it expands increases, causing a slower expansion. Figure 4 shows the shock front position plotted against the inverse third power of the ambient gas pressure. Here θ is the angle between the incoming laser

direction and the radial cord measured. For $\theta = 45^o$ and $\theta = 15^o$ (both outside the laser entrance cone) the data are described well by a straight line fit. At $\theta = 0^o$ the fit is less good due to the modification of the shock front by the laser passage in this region.

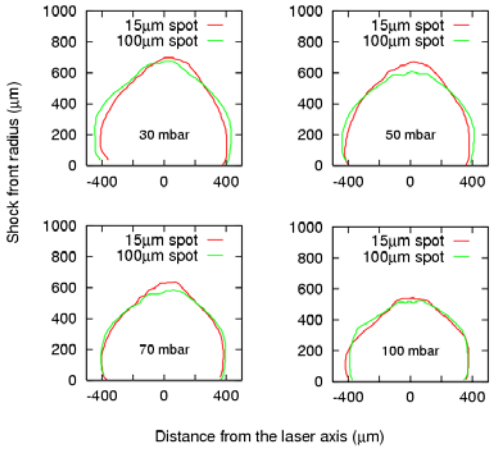

Figure 3. Shock front positions at a probe delay of 4ns. Changing the focal spot size affects the propagation of the shock wave in the direction back along the laser axis. This is particularly apparent for the 50mbar and 70mbar cases.

From the interferometric data, one-dimensional n_e profiles can be inferred. These profiles represent the line integral of n_e along the path taken by the probe beam through the plasma. The minimum value for the change in n_e that can be measured with this method is dependent upon the probe laser wavelength, and the length of plasma through which the laser propagates, and is ~ $2x10^{18}$ cm^{-3} in the case of an 800µm plasma and 400nm laser wavelength. Because of the spherical geometry of the system, the sensitivity of this diagnostic decreases further away from the target surface (since the probe propagates through a decreasing length of plasma).

Figure 5 shows the inferred one-dimensional n_e profiles moving away from the target surface along the drive laser axis. These data were taken at a probe delay of 4ns and a focal spot size of 100µm. No density jump could be observed at a gas pressure of 10mbar as it was below the minimum sensitivity of the instrument.

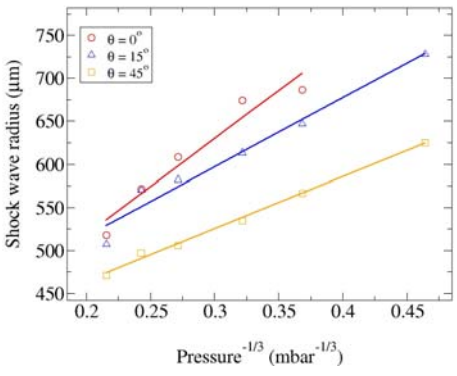

Figure 4. Shock front position as a function of the inverse cube of the ambient gas pressure, see text for details. The error bars are smaller than the data points.

The shock front can clearly be seen as a peak in the n_e profile. The swept-up mass, and hence the density, is greater for higher ambient gas pressures. In a collisional shock, the thickness of the shock front is of the order of the collisional mean free path of particles in the shock front. Increasing the background gas pressure decreases the particle mean free path of the system, and so it is expected that the shock front should be thinner for the higher gas pressures. This is consistent with the data presented in Figure 5.

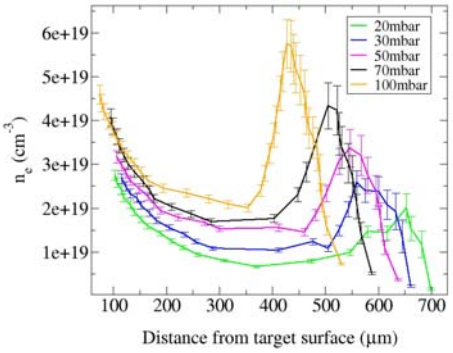

Figure 5. One-dimensional inferred n_e profiles along the incoming drive laser axis, recorded at 4ns and with a 100µm focal spot. At higher ambient pressures the density of the shock front is increased and the shock thickness is decreased.

Discussion

In all cases the propagation of the shock wave is clearly modified in the direction back along the drive laser beam. The probe times of interest (up to 13ns) are more than 1000 times longer than the duration of the pulse (3ps); hence this modification is not a result of a direct laser-shock interaction. Instead, it appears that the physical properties of the background gas are changed by the laser's passage.

From Figures 3 and 5, it is clear that the shock travels faster in a lower density gas. From shadowgrams at 4ns (see Figure 3) and at 13ns, it is seen that the shock wave travels faster in, and very close to, the incoming laser cone, resulting in a bump in the shock front profile. It is therefore suggested that the incoming laser creates a low-density channel in the ambient gas, which exists for a period of time long enough to modify the shock wave dynamics. This density channel is not seen in the interferograms, and so an upper limit can be place on the magnitude of the perturbation; it must be smaller than the sensitivity of the diagnostic. The maximum distance from the target surface which could be seen with the interferometer was ~1000µm. In the region between the edge of the field of view and the shock front (~ 500µm from the target surface) the converging laser beam has a diameter of between 170µm - 90µm for a 15µm focal spot, and 255µm - 175µm for a 100µm focal spot. The minimum n_e change that can be observed along a chord of length equal to the laser beam diameter is therefore $8x10^{18}$ cm^{-3} – $2x10^{19}$ cm^{-3} for a 15µm focal spot, and $6x10^{18}$ cm^{-3} – $8x10^{19}$ cm^{-3} for a 100µm focal spot.

It is clear that in order to fully understand the shock wave behaviour, the physical conditions in the ambient gas must be better understood. This ambient gas can be divided into two regions – gas that is far from the laser entrance cone, which is weakly photoionised by x-rays generated in the laser-solid target interaction, and gas in the region around the laser cone, which first interacts with the incoming laser before the arrival of the x-ray flux. Future experiments could employ an optical spectrometer coupled to a gated CCD camera. This would provide spatially, spectrally and temporally resolved data, which would allow measurement of the level of ionisation of the ambient nitrogen due to x-rays from the target, as well as any ionisation of the gas resulting from the passage of the laser.

References

1. J Grun, *et al.*, Phys. Rev. Lett. 66, 2738 (1991)
2. T Ditmire, *et al.*, Astro. J. Supp. 127, 299 (2000)
3. M J Edwards, *et al.*, Phys. Rev. Lett. 87, 085004 (2001)
4. A D Edens, *et al.*, Phys. Plasmas. 11, 4968 (2004)